

Some optical and dielectric properties of spray deposited tin oxide thin films

H. M. ALI^a, E. KH. SHOKR^a, A. V. MARCHENKO^b

^aPhysics Department, Faculty of Science, Sohag University, 82524 Sohag-Egypt

^bAlexander Herzen State Pedagogical University of Russia, 191186, St. Petersburg, Russia

Transparent conducting tin oxide thin films have been deposited by spray pyrolysis technique. The effect of substrate temperature on the structure and optical properties of tin oxide thin films has been studied. The increase in the substrate temperature led to increase the optical transmission. A transmittance value of 84% has been obtained for spray-deposited film at 400 °C. The absorption coefficient which is used to determine the optical band gap, real dielectric constant and free carrier concentration has been calculated using four equations. An increase in the band gap and the free carrier concentration were observed by increasing the substrate temperature during deposition from 200 to 400 °C.

(Received October 29, 2012; accepted April 11, 2013)

Keywords: Transmittance, Optical energy gap, Real dielectric constant, Free carrier concentration

1. Introduction

Transparent conducting oxides (TCOs), have received much attention because of their wide applications in the field of optoelectronic devices [1-8].

Tin oxide is an n-type semiconductor material with wide band gap energy from 3.4 to 4.0 eV [9, 10]; it has high donor concentration and large mobility [11]. Tin oxide thin films can be used in various applications such as gas sensors [12], transistors, electrocatalytic anodes [13], solar cells [14], catalysts [15, 16] and electrochromic devices [17]. Tin oxide thin films have been deposited by various techniques such as spray pyrolysis [18], magnetron sputtering [19], chemical vapour deposition [20, 21], sol-gel spin coating [20], evaporation-condensation method [22] and dip coating [23, 24] techniques.

The spray pyrolysis technique is a simple, economical and highly feasible process in which a thin film is deposited by spraying a solution on heated substrate. This technique has been used to deposit good quantity doped and undoped thin films [25].

In this study, the effect of substrate temperature during deposition on the structure and optical properties of spray-deposited tin oxide films from the initial solution of tin dichloride ($\text{SnCl}_2 \cdot 2\text{H}_2\text{O}$) in ethanol has been investigated. On the other hand, four equations for determining the absorption coefficient have been used to determine the optical band gap, real dielectric constant and free carrier concentration.

2. Experimental details

Thin films of tin oxide were prepared by spray pyrolysis technique. A solution of commercial tin dichloride ($\text{SnCl}_2 \cdot 2\text{H}_2\text{O}$) was prepared by dissolving the required quantity of tin dichloride in pure ethanol. The starting solution was sprayed through a pneumatic nozzle

of simple sprayer onto the ultrasonically cleaned glass substrates (the transmittance of glass substrate ~ 91% either in the visible or near infrared regions). The glass substrates have been ultrasonically cleaned by means of ultrasonic cleaner instrument model (1210) using acetone and distill water. The substrates were heated for 5 min before deposition. The substrate temperature during deposition was maintained at $T_s = 200, 250, 300, 350$ and 400 °C. Deposition time and nozzle to substrate distance were kept constant at 30 cm. There are different methods for determining the film thickness such as optical methods, mechanical stylus method [26], using detectors [27], profilometers [28] or weight difference method [29]. In this work, the thickness of the deposited thin film was determined using the following Eq. [30, 31]:

$$d = \frac{m}{\rho A} \quad (1)$$

where m is the mass of the thin film deposited onto the substrate, A the area of the deposition of the film, d the film thickness and ρ is the density of tin oxide which is assume to be the same as that of the bulk material. The thickness of the films is found to equal ~ 152 - 172 nm.

Investigations of the microstructure were carried out using an X-ray diffractometer (X' Pert Philips, Holland) Cu-K_α diffractometer ($\lambda = 1.541838$ Å).

A Jasco V-570 UV-visible-NIR spectrophotometer (with photometric accuracy of ± 0.002 – 0.004 absorbance and $\pm 0.3\%$ transmittance) was employed to record the transmission and reflection spectra over the wavelength range 200-2500 nm at normal incidence.

3. Results and discussion

Fig. 1 shows the variation of film thickness of spray-deposited tin oxide films with substrate temperature. It is shown that the thickness of films decrease with increasing

the temperature of substrate, which can be interpreted as due to the decrease in interstitial water molecules [32].

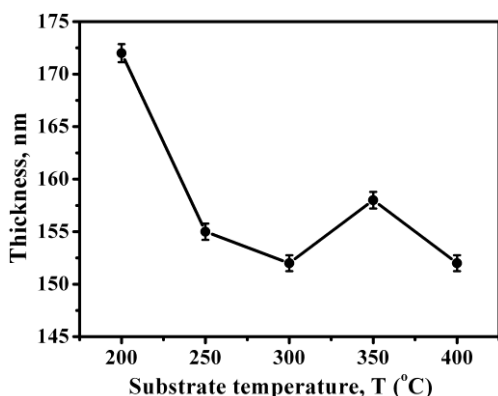


Fig. 1. Variation of film thickness of spray-deposited tin oxide films versus substrate temperature

The XRD patterns of spray-deposited tin oxide films deposited at various substrate temperatures are shown in Fig. 2. It is observed that, the spray-deposited film at 250 °C exhibits an amorphous nature, whereas the films deposited at 350 and 400 °C exhibit polycrystalline structure, displaying the prominent diffraction peaks at $2\theta = 25.01$, 41.6 and 72.4° corresponding to SnO_2 (111), (211) and (324) crystal planes, respectively. Another two diffraction peaks corresponding to the SnO (110) and (112) were observed at $2\theta = 23.4$ and 28.9° . The presence of SnO and SnO_2 means that Sn exists in two oxidation states, Sn^{2+} and Sn^{4+} , respectively. The intensity of diffraction peaks increases with increasing the substrate temperature, indicating to the enhancement of the film crystallinity.

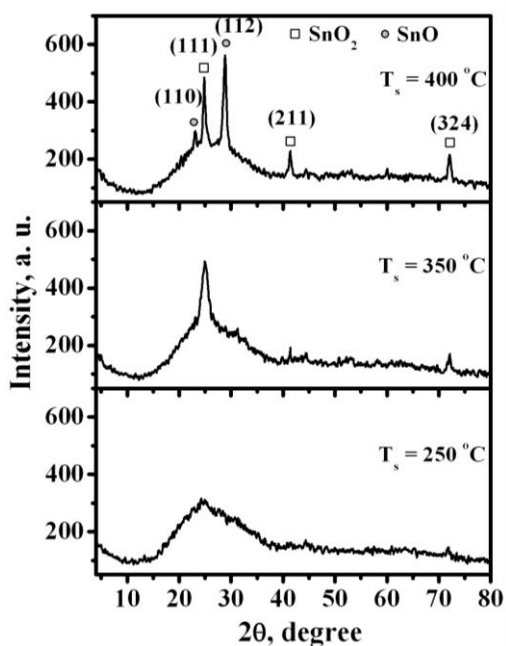


Fig. 2. XRD patterns of spray-deposited tin oxide thin film at various substrate temperatures.

The typical UV-VIS –NIR optical transmittance spectra of tin oxide films deposited at different substrate temperature as a function of wavelength in the range from 300 to 2500 nm are shown in Fig. 3-a. It is evident that the transmittance increases with increasing the substrate temperature and the maximum value of transmittance in the visible region $\sim 84\%$ has achieved for tin oxide film deposited at 400 °C. The average values of transmittance in the visible (T_{vis}) and near infrared (T_{IR}) regions are shown in Fig. 3-b. In general, the transmittance of films is depending mainly on three factors: (1) oxygen deficiency, (2) surface roughness and (3) impurity centers [7]. In our case, the increase in transmittance of tin oxide film with increasing the substrate temperature is due to the decrease of the impurity centers and / or the relatively increase of corporation with oxygen. It is seen also that the absorption edge shifts towards shorter wavelength, suggesting a widening of the energy band-gap with increasing substrate temperature.

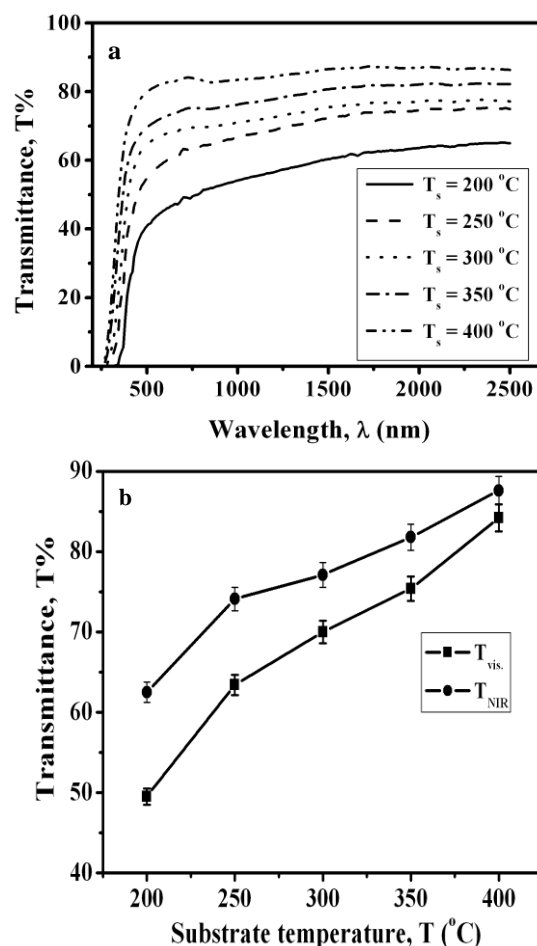


Fig. 3. (a) Spectral variation of the transmittance T with wavelength. (b) Variations of the transmittance in the visible and near infrared region for spray-deposited tin oxide thin films with substrate temperatures.

From the literature survey, it was found that the absorption coefficient can be calculated by a series of equations [33–36] using the transmittance and reflectance readings as follows:

$$\alpha_1 = \frac{2.303}{d} \log_{10} \left(\frac{1}{T} \right) \quad (2)$$

$$\alpha_2 = \frac{2.303}{d} \log_{10} \left(\frac{1-R}{T} \right) \quad (3)$$

$$\alpha_3 = \frac{2.303}{d} \log_{10} \left(\frac{(1-R)^2}{T} \right) \quad (4)$$

$$\alpha_4 = \frac{2.303}{d} \log_{10} \left[\frac{(1-R)^2 + \sqrt{(1-R)^4 + (2RT)^2}}{2T} \right] \quad (5)$$

where d , R and T are the film thickness, reflectance and transmittance, respectively.

Previous researchers put conditions for using each equation. Here we will examine these equations (2-5) for calculating the optical energy gap, the real dielectric constant, residual dielectric constant and the free carriers' concentration for spray deposited SnO_2 , neglecting all

conditions of using any of these equations.

Using the optical absorption coefficient α calculated using equations (2-5), evaluated from the optical transmission and reflection data of tin oxide films, the allowed direct band gap E_g values were obtained by extrapolating the linear portion of the plots of $(\alpha hv)^2$ versus hv to $\alpha = 0$ [37] as shown in Fig. (4-a, b, c, d, e). The dependence of optical band gap on substrate temperature is shown in Fig. 4-f. It is evident that the magnitudes of the optical energy gaps, which were obtained using the different above equations, are approximately the same and the deviations are in the range of error bars. It is shown also that the optical band gap increases with increasing the substrate temperature to reach its maximum value of 4.5 eV for tin oxide film deposited at 400 °C. The increase in optical energy gap can be attributed to the Burstein–Moss shift; as carriers fill the states at the bottom of the conduction band, the Fermi level rises and the optical gap increases [38] (this can be confirmed by Fig. 7).

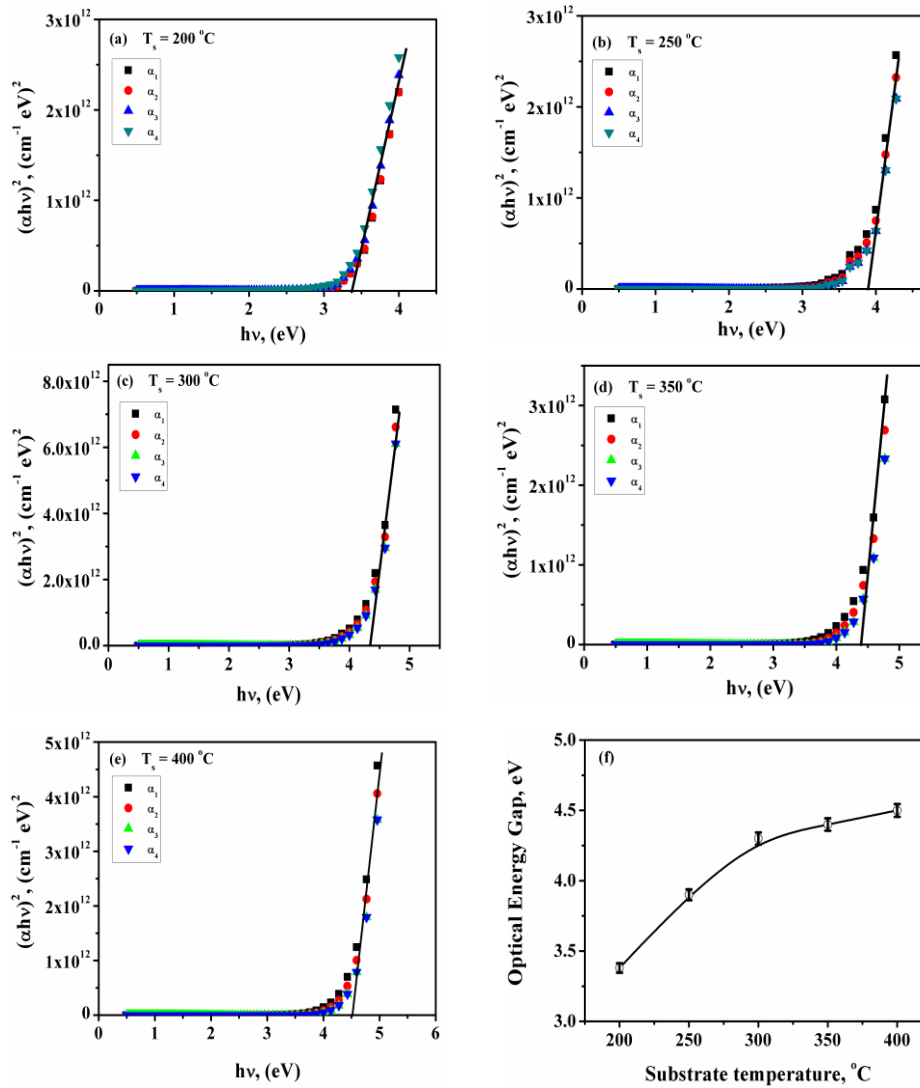


Fig. 4. Plots of $(\alpha hv)^2$ versus hv (where α were calculated from equations 2-5) (a, b, c, d, e) and plot of the optical band gap E_g (f) for spray-deposited tin oxide thin films at various substrate temperatures.

In the exponential part of the absorption edge, the absorption coefficient is governed by the Urbach relation [39].

$$\alpha(h\nu) = \alpha_0 \exp\left(\frac{h\nu}{E_u}\right) \quad (6)$$

where α_0 is a constant and E_u is the Urbach energy which is interpreted as the width of tails of localized states in the gap region and in general represents the degree of disorder in the amorphous semiconductor. The Urbach energy, E_u values were calculated from the inverse of the slope of the straight line of the relation $\ln \alpha$ vs. $h\nu$. The corresponding values of the Urbach energy are shown in Fig. 5. It is evident that the Urbach energy increases with increasing the substrate temperature up to 300 °C and then decreased at higher substrate temperature. The increase of the Urbach energy up to 300 °C can be attributed to the increase of disorder at low substrate temperature due to the amorphous nature of the films [40]. The decrease in the Urbach energy above substrate temperature of 300 °C is due to the decrease in the density of localized states as a result to the enhancement of the film crystallinity as shown in Fig. 2.

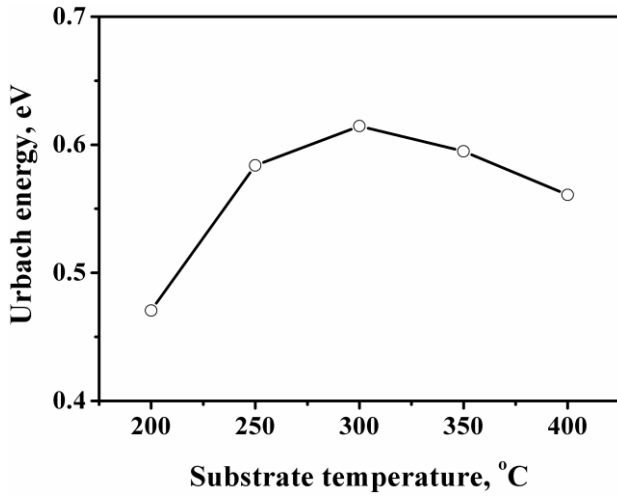


Fig. 5. Plot of Urbach energy as a function of substrate temperature.

The real dielectric constant ϵ' , which is resulted due to the contribution from the free carrier electric susceptibility was determined using the Drude's theory of dielectrics, which is given from the following eq. [16]:

$$\epsilon' = n^2 - k^2 = \epsilon_i - \frac{e^2}{\pi c^2} \left(\frac{N_{opt}}{m^*} \right) \lambda^2 \quad (7)$$

where n is the refractive index, calculated from the optical reflection as follows [41]

$$n = \frac{\left(1 + R^{1/2}\right)}{\left(1 - R^{1/2}\right)} \quad (8)$$

$k = \alpha\lambda/4\pi$ is the extinction coefficient, ϵ_i is the infinitely high frequency dielectric constant or the residual dielectric constant due to the ion core, N_{opt}/m^* is the ratio of carrier concentration to the effective mass and e is the elementary charge (1.6×10^{-19} C).

Since the extinction coefficient k is a function in absorption coefficient α , so the real dielectric constant is examined and determined using the previous four equations (2-5) as shown in Fig. 6-a, b, c, d, e and the corresponding residual dielectric constant ϵ_i , is shown in Fig. 6-f. Table 1 illustrates the intercepts and slopes of the fit linear relations between the real dielectric constant ϵ' vs. wavelength square λ^2 in the near infrared region. It is shown that the values of either slopes and/or intercepts for each film prepared at fixed substrate temperature are approximately the same. On the other hand, as shown in Fig. 6-f, the four points of the residual dielectric constant, ϵ_i , which are determined from the intercepts of the relation between the real dielectric constant vs. wavelength square λ^2 using different absorption coefficient equations $\alpha_1, \alpha_2, \alpha_3, \alpha_4$ are identical. The Drude's theory of dielectrics was used also to calculate the values of carrier concentration N_{opt} from the optical data. The variations in carrier concentration N , are shown in Fig. 7. It is clear that, the four curves resulting from using the four above equations of absorption coefficient (2-5) are identical. It is shown also that the carrier concentration increases with increasing the substrate temperature which can be attributed to the presence of two oxidation states for tin Sn^{4+} and Sn^{2+} indicating to the incomplete oxidation of the films and to the chlorine contamination [42].

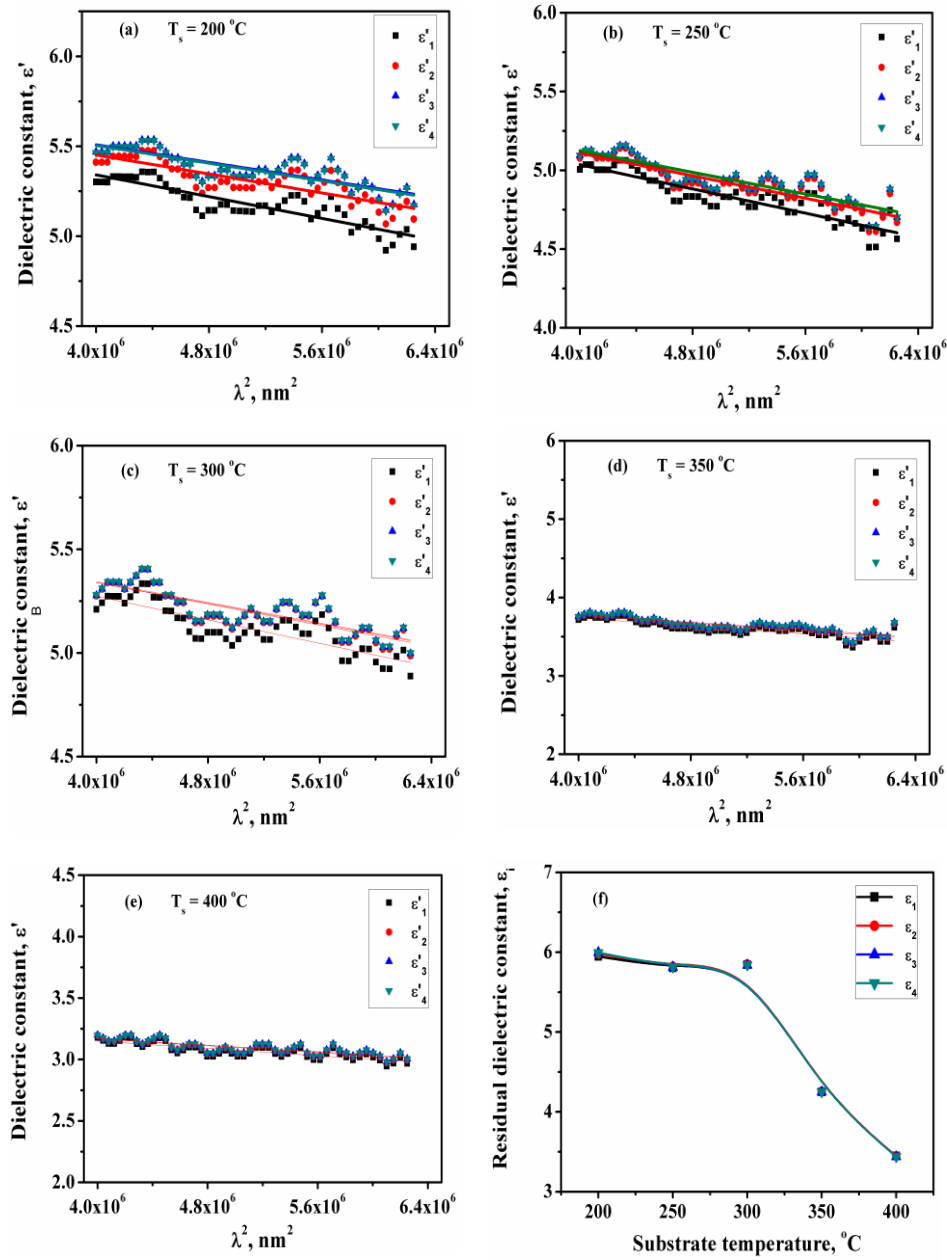


Fig. 6. Plots of dielectric constant ϵ' versus λ^2 (where a were calculated from equations 2-5) (a, b, c, d, e) and plot of the residual dielectric constant ϵ_i (f) for spray-deposited tin oxide thin films at various substrate temperatures.

Table 1. The intercepts and slopes of the fit linear of the relations between the real dielectric constant ϵ' and the wavelength square λ^2 in the near infrared region.

	$T_s = 200^\circ\text{C}$		$T_s = 250^\circ\text{C}$		$T_s = 300^\circ\text{C}$		$T_s = 350^\circ\text{C}$		$T_s = 400^\circ\text{C}$	
symbol	Intercept	Slope								
ϵ_1	5.947	-1.51×10^{-7}	5.804	-1.92×10^{-7}	5.843	-1.42×10^{-7}	4.249	-1.28×10^{-7}	3.446	-7.42×10^{-7}
ϵ_2	5.980	-1.32×10^{-7}	5.822	-1.78×10^{-7}	5.851	-1.28×10^{-7}	4.256	-1.21×10^{-7}	3.446	-6.96×10^{-7}
ϵ_3	5.996	-1.22×10^{-7}	5.812	-1.72×10^{-7}	5.838	-1.25×10^{-7}	4.249	-1.18×10^{-7}	3.438	-6.71×10^{-7}
ϵ_4	5.995	-1.23×10^{-7}	5.815	-1.72×10^{-7}	5.842	-1.24×10^{-7}	4.251	-1.18×10^{-7}	3.439	-6.72×10^{-7}

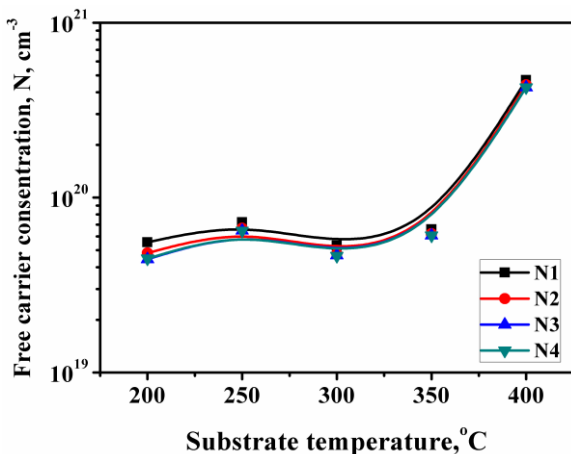


Fig. 7. Variation of the carrier concentration for spray-deposited tin oxide thin films at various substrate temperatures.

4. Conclusion

Tin oxide thin films have been prepared by dissolving dichloride ($\text{SnCl}_2 \cdot 2\text{H}_2\text{O}$) in pure ethanol and deposited by spray pyrolysis technique. The effect of substrate temperature on the structure and optical properties of tin oxide thin films has been studied. It was found that, the increase in the substrate temperature led to increase the optical transmission. The maximum value of transmittance (exceed 84%) in the visible region has been obtained for spray-deposited tin oxide film at substrate temperature of 400 °C. An increase in the band gap (3.38 - 4.5 eV) and the free carrier concentration (4.8×10^{19} - $4.41 \times 10^{20} \text{ cm}^{-3}$) were observed by increasing the substrate temperature during deposition from 200 to 400 °C.

The absorption coefficient which is used to determine the optical band gap, real dielectric constant and free carrier concentration has been calculated using four equations (2-5). It was found that at fixed substrate temperature, the magnitudes of the obtained optical energy gap which was derived from the different equations are approximately the same and the deviations in magnitude are in the range of error bars. The same behavior was also observed for residual dielectric constant and free carrier concentration.

Acknowledgements

The author would like to thank Dr. A. A. Amer Chemistry Dept. Faculty of Science, Sohag University for fruitful helping during the preparation of the chemical solution.

References

[1] E. Kh. Shokr, M. M. Wakkad, H. A. Abd El-Ghanny,

- H. M. Ali, *J. Phys. Chem. Solids*, **8**, 75 (2000).
 [2] H. Kim, A. Pique, J. S. Horwitz, H. Murata, Z. H. Kafafi, C. M. Gilmore, D. B. Chrisey, *Thin Solid Films* **377-378**, 798 (2000).
 [3] H. M. Ali, *phys. stat. sol. (a)* **202**(14), 2742 (2005).
 [4] E. J. J. Martin, M. Yan, M. Lane, J. Ireland, C. R. Kannewurf, R. P. H. Chang, *Thin Solid Films* **461**, 309 (2004).
 [5] Michio Mikawa, Toshihiro Moriga, Yuji Sakakibara, Yukinori Misaki, Kei-ichiro Murai, Ichiro Nakabayashi, Kikuo Tominaga, *Materials Research Bulletin* **40**, 1052 (2005).
 [6] H. M. Ali, M. M. Abd El-Raheem, N. M. Megahed, H. A. Mohamed. *J. Phys. Chem. Solids* **67**, 1823 (2006).
 [7] H. M. Ali, H. A. Mohamed, M. M. Wakkad, M. F. Hasaneen, *Thin Solid Films* **515**, 3024 (2007).
 [8] H. A. Mohamed, H. M. Ali, *Sci. Technol. Adv. Mater.* **9** (2008).
 [9] L. S. Roman, R. Valaski, C. D. Canestraro, E. C. S. Magalhaes, C. Persson, R. Ahuja, E. F. da Silva Jr., I. Pepe, A. Ferreira da Silva, *Appl. Surf. Sci.* **252**, 5361 (2006).
 [10] Rajaram S. Mane, Jinho Chang, Dukho Ham, B. N. Pawar, T. Ganesh, Byung Won Cho, Joon Kee Lee, Sung-Hwan Han, *Current Applied Physics* **9**, 87 (2009).
 [11] Z. M. Jarzebski, J. P. Marton, *J. Electrochem. Soc.* **123** (1976) 199C, 299C, 333C.
 [12] P. Mwnini, F. Parret, M. Guerrero, K. Soulantica, L. Erades, A. Maisonnat, B. Chaudret, *Sen. Actuators, B, Chem.* **103** (2004).
 [13] P. Duverneuil, F. Maury, N. Pebere, F. Senocq, H. Vergnes, *Surf. Coat. Technol.* **151-152**, 9 (2002).
 [14] M. A. El Khakani, R. Dolbec, A. M. Serbenti, M. C. Horrillo, M. Trudeau, R. G. Saint-Jacques, D. G. Rickerby, I. Sayago, *Sens. Actuators, B, Chem.* **87**, 321 (2002).
 [15] T. Tagawa, S. Kataoka, T. Hattori, Y. Murakami, *Appl. Catal.* **4**, 1 (1994).
 [16] P. W. Park, H. H. Kung, D. W. Kim, M. C. Kung, *J. Catal.* **184**, 440 (1999).
 [17] Ji-Hyoen Im, Jae-Ho Lee, Dong-Wha Park, *Surface & Coatings Technology* **202**, 5471 (2008).
 [18] K. Ueda, T. Hase, H. Yanagi, H. Kawazoe, H. Honoso, M. Ohata, M. Hirano, *J. Appl. Phys.* **89**, 1790 (2001).
 [19] Z. C. Jin, L. Hamberg, J. Granqvist, *Appl. Phys.* **64**, 5117 (1988).
 [20] O. F. Khan, P. O'Brien, *Thin Solid Films* **173**, 95 (1989).
 [21] M. Toyoda, J. Watanabe, T. Matsumiya, *J. Sol-Gel Sci. Technol.* **1**, 93 (1999).
 [22] S. H. Mohamed, *Journal of Alloys and Compounds* **510**, 119 (2012).
 [23] M. Ohyama, *J. Am. Ceram. Soc.* **81**, 1622 (1998).
 [24] M. J. Alam, D. C. Cameron, *J. Vac. Sci. Technol. A* **19**, 1642 (2001).

- [25] A. V. Moholkar, S. M. Pawar, K. Y. Rajpure, P. S. Patil, C.H. Bhosale, *J. Phys. Chem. Solids* **68**, 1981 (2007).
- [26] M. de la L. Olvera, H. Gómez, A. Maldonado, *Solar Energy Materials and Solar Cells*, **91**, 1449 (2007).
- [27] Chitra Agashe, Shailaja Mahamuni, *Thin Solid Films* **518**, 4868 (2010).
- [28] M. A. Lucio-Lo´pez, A. Maldonado, R. Castanedo-Pe´rez, G. Torres-Delgado, M. de la L. Olvera, *Solar Energy Materials & Solar Cells* **90**, 2362 (2006).
- [29] P. S. Patil, S. H. Mujawar, S. B. Sadale, H. P. Deshmukh, A. I. Inamdar, *Materials Chemistry and Physics* **99**, 309 (2006).
- [30] P. K. Pandey, N. S. Bhave, R. B. Kharat, *Ind. J. Chem.* **44A**, 2034 (2005).
- [31] D. W. Ma, Z. Z. Ye, J. Y. Huang, L. P. Zhu, B. H. Zhao, J. H. He, *Materials Science and Engineering B* **111**, 9 (2004).
- [32] H. M. Ali, M. M. Abou-Mesalam, M. M. El-Shorbagy, *Journal of Physics and Chemistry of Solids*, **71**, 51 (2010).
- [33] M. Rusop, K. Uma, T. Soga, T. Jimbo, *Materials Science and Engineering B* **127**, 150 (2006).
- [34] W. Q. Hong, *J. Phys. D: Appl. Phys.* **22**, 1384 (1989).
- [35] M. Becker, H. Y. Fan, *Phys. Rev.* **76** 1530, 40 (1949).
- [36] J. I. Pankove, *Optical Processes in Semiconductors*, Dover Publications, Inc., NY, 1971.
- [37] Prashant Kumar Pandey, N. S. Bhave, R. B. Kharat, *Electrochimica Acta* **51**, 4659 (2006).
- [38] E. Burstein, *Phys. Rev.* **93**, 632 (1954).
- [39] F. Urbach, *Phys. Rev.* **92**, 1324 (1953).
- [40] N. A. Hegab, A. E. Bekheet, M. A. Afifi, A. A. El-Shazly, *Appl. Phys. A* **66**, 235 (1998).
- [41] R. Bhat, P. S. Dutta, S. Guha, *Journal of Crystal Growth* **310**, 1910 (2008).
- [42] R. R. Kasar, N. G. Deshpande, Y. G. Gudage, J. C. Vyas, Ramphal Sharma, *Physica B* **403**, 3724 (2008).
- [43] G. Haacke, *J. Appl. Phys.*, **47**, 4086 (1976).

*Corresponding author: hazem95@yahoo.com